Reentrant cluster glass and stability of ferromagnetism in the Ga_2MnCo Heusler alloy

Tamalika Samanta,[1] P. A. Bhobe,[1,2,*] A. Das,[3] A. Kumar,[3] and A. K. Nigam[4]

[1]*Department of Metallurgy Engineering and Materials Science, Indian Institute of Technology Indore, Simrol, Indore 453 552, India*

[2]*Discipline of Physics, Indian Institute of Technology Indore, Simrol, Indore 453 552, India*

[3]*Solid State Physics Division, Bhabha Atomic Research Centre, Mumbai 400 085, India*

[4]*Tata Institute of Fundamental Research, Homi Bhabha Road, Mumbai 400 005, India*

(Received 3 March 2018; published 18 May 2018)

We present here a detailed investigation into the magnetic ordering of a full Heusler alloy Ga_2MnCo using dc and ac magnetization measurements, neutron diffraction, and neutron depolarization experiments. The crystal structure at room temperature was first confirmed to be $L2_1$ using the highly intense synchrotron x-ray diffraction technique. Temperature-dependent magnetization reveals that Ga_2MnCo enters a ferromagnetic (FM) state at $T_C = 154$ K, characterized by a sharp increase in magnetization and a plateaulike region hereafter. As the temperature is decreased further, a sharp drop in magnetization is observed at $T_f = 50$ K, hinting toward an antiferromagnetic (AFM) phase change. Neutron diffraction (ND) recorded over the range of temperature from 6 to 300 K provides combined information regarding crystal as well as magnetic structure. Accordingly, an increase in the intensity of the ND pattern is seen at 150 K, signaling the onset of long-range FM order. However, there is no sign of the appearance of superlattice reflections corresponding to the AFM phase in the patterns recorded below 50 K. An unusual discontinuity in the unit-cell volume is seen around T_f, indicating a coupling of this second transition with the contraction of the lattice. Attempts to unravel this interesting magnetic behavior using ac susceptibility measurements led to the existence of glassy magnetism below T_f. Systematic analysis of the susceptibility results along with neutron depolarization measurement identifies the low-temperature phase as a reentrant cluster glass.

DOI: 10.1103/PhysRevB.97.184421

I. INTRODUCTION

Generally, full Heusler alloys are of the chemical form X_2YZ, where X and Y are transition metals and Z is a main group element belonging to the s and p blocks. The crystallographic positions available to these atoms are $A(\frac{3}{4},\frac{3}{4},\frac{3}{4})$, $B(\frac{1}{2},\frac{1}{2},\frac{1}{2})$, $C(\frac{1}{4},\frac{1}{4},\frac{1}{4})$, and $D(0,0,0)$. Accordingly, $L2_1$ structure is realized when the X atom occupies A and C sites, the Y atom occupies the B site, and the Z atom is present at the D site resulting in $XYXZ$ order. The presence of two magnetic sublattices in a full Heusler system often results in magnetic interactions such as antiferromagnetism, ferrimagnetism, and compensated ferrimagnetism to localized-itinerant ferromagnetism including a complex spin glass state [1–4]. Hence apart from being technologically useful, they are ideal systems to study the nature of magnetic correlations in diverse magnetically ordered states. Unlike such a standard Heusler form, the Ga_2MnCo composition has an sp element in excess with two parts of Ga to one part each of Mn and Co, reversing the general chemical formula to Z_2XY, yet maintaining the $L2_1$ structural form.

Very few examples of such Z_2-based systems exist, including the ferromagnetic shape memory alloy Ga_2MnNi with a martensitic transformation at 780 K and a Curie temperature at 330 K [5] and Al_2MnCo [6] with a reentrant spin-glass behavior and a dominating ferromagnetic coupling between transition metals. First-principles electronic-structure calculations have also been performed on isostructural alloying of Ga_2MnCo-Ga_2MnV alloys, where the exchange interaction between Mn and V atoms is found to change from antiferromagnetic to ferromagnetic coupling with increasing ratio of the lattice constants, c/a [7]. This gives an important indication of finding a myriad of unusual magnetic and structural properties on exploring new Z_2-based Heusler alloys.

Magnetism in Ga_2MnCo is considered to be of ferrimagnetic type, originating from the antiparallel aligned moments of Mn and Co sublattices [7,8]. The other two Heusler compositions in the Co-Mn-Ga alloys, viz., Co_2MnGa ($L2_1$) and Mn_2CoGa (Hg_2CuTi), show strong ferromagnetic and soft ferrimagnetic behavior, respectively [9,10]. In fact, in Ref. [8], a magnetic compensation behavior was found with systematic substitution of Ga in Co_2MnGa as the chemical composition changed from Co_2MnGa to Ga_2MnCo and was conjectured to be due to the competitive nature of the Co and Mn moments. Furthermore, band-structure studies reveal a stronger covalent hybridization between the p electrons of the main group of Ga atoms and d electrons of transition-metal atoms. This hybridization is believed to cause a higher density of states (DOS) near the Fermi level (E_F), and subsequently lead to an unstable magnetic configuration [8].

Early work on $GaCo_{1-x}Mn_x$ ($x = 0$–0.55) pseudobinary compositions [11] claimed it to be a reentrant spin glass based on ac magnetic susceptibility measurements carried out under dc magnetic fields. It may be noted that the investigated compositions were not in a 2 : 1 : 1 Heusler ratio. Atomic

*pbhobe@iiti.ac.in

disorder does lead to a *glassy* magnetic state in many systems [12] and can coexist with an exotic ground state such as superconductivity, as found in pseudobinary intermetallic compounds [13]. Other example includes the giant exchange bias field with the reentrant spin-glass–FM interface caused by antisite disorder in Mn atoms in a $Mn_2Ni_{1.6}Sn_{0.4}$ Heusler alloy [14]. Such glassy behavior (mostly noncanonical) with exceptional functional properties has led to a resurgence of attention in this area. Thus it appears that the problem of magnetic order in Ga_2MnCo has a nontrivial interest in its own right since there exist excess main group atoms, in addition to two magnetic atoms, that play a significant role in the formation of the magnetic ground state.

With an aim to obtain a deeper perspective about magnetic correlations in Ga_2MnCo, we have carried out a thorough investigation into its crystal structure and its magnetic and electrical transport properties. A combination of high-resolution synchrotron x-ray diffraction and neutron diffraction study clarifies the crystal structure and exact site occupancies of the magnetic ions in Ga_2MnCo. dc magnetization and the neutron depolarization measurements carried out as a function of temperature identify the distinctive magnetic phase-transition temperatures. Temperature variation of ac susceptibility unravels the low-temperature glassy phase. In this paper, we discuss the role of magnetic ions in pushing the system toward a glassy magnetic state at low temperatures even after ordering as a ferromagnet at higher temperatures.

II. EXPERIMENTAL DETAILS

A polycrystalline bead of Ga_2MnCo (6.5 g) was prepared by arc-melting the starting elements ($\geqslant$99.99% purity) under an argon atmosphere. To ensure good homogeneity, the bead obtained after first melting was flipped over and remelted several times, ensuring minimum weight loss. The homogeneous bead so obtained was sealed in an evacuated quartz tube and annealed at 800 °C for 7 days before quenching in ice water. The phase purity of the sample was checked by powder diffraction recorded at room temperature using synchrotron radiation ($\lambda = 0.9782$ Å) at Indian beamline, BL18B, Photon Factory, KEK, Japan. Energy-dispersive x-ray analysis (EDXA) using a SUPRA 55 Zeiss field-emission scanning electron microscope confirms the homogeneity of the sample. The elemental ratio 51.4 : 25 : 23.7 for Ga : Mn : Co represents an average value (with a standard deviation of 3%) obtained after recording several EDX spectra from different spatial locations on the sample. The four-probe electrical resistivity measurements were carried out using the transport properties option of the physical properties measurement system of Quantum Design, Inc. The magnetization measurement was done using a superconducting quantum interference device (SQUID) -based magnetometer by Quantum Design, Inc. The ac susceptibility as a function of temperature was measured at various frequencies using a physical properties measurement system. Neutron diffraction patterns were recorded on the PD2 powder neutron diffractometer ($\lambda = 1.2443$ Å) at the Dhruva reactor, Bhabha Atomic Research Centre, Mumbai, India. Neutron depolarization measurements were carried out on the Polarized Neutron Spectrometer at Dhruva reactor.

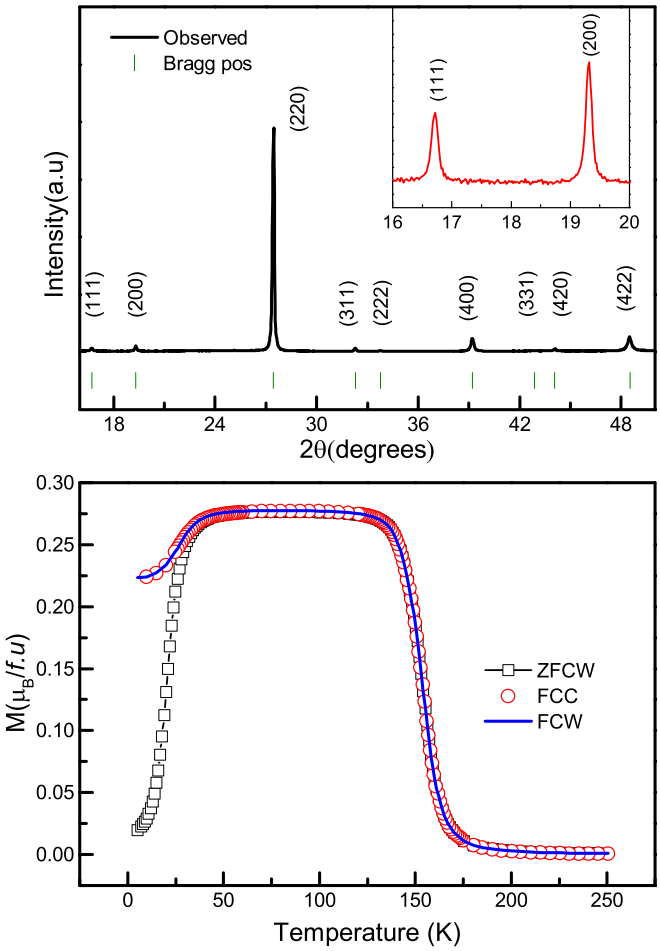

FIG. 1. Structural and magnetic properties of Ga_2MnCo. (a) The room-temperature synchrotron powder XRD pattern of Ga_2MnCo. The bars show the Bragg positions. Inset: magnified view of the (111) and (200) superlattice reflections. (b) Temperature dependence of magnetization of Ga_2MnCo in an applied magnetic field of 100 Oe.

III. RESULTS

Ga_2MnCo was examined for its crystal structure using high-resolution synchrotron x-ray powder diffraction (XRD) with wavelength $\lambda = 0.9782$ Å. The XRD profile recorded at room temperature is presented in Fig. 1(a). All the observed peaks are indexed to a face-centered-cubic cell in the $Fm\bar{3}m$ space group, confirming the phase purity of the sample. In addition to the principal reflection peaks of the (220), (400), and (422) planes, the fcc-typical superlattice reflections of the (111) and (200) planes are also present (see the inset), indicating Ga_2MnCo to be a well-ordered, single-phase system with a cubic $L2_1$ structure. However, the intensity of these reflections is adversely affected due to similar x-ray scattering factors for Mn and Co atoms. The $L2_1$ structure is described as four interpenetrating fcc sublattices with X atoms occupying the 8c Wyckoff positions (0.25,0.25,0.25), and Y and Z atoms located in the 4b site (0.5,0.5,0.5) and the 4a site (0,0,0), respectively. Hence, the presence of (111) and (200) peaks signifies a highly ordered $L2_1$ lattice. Further, from the XRD pattern we estimate the lattice parameter of the sample to be

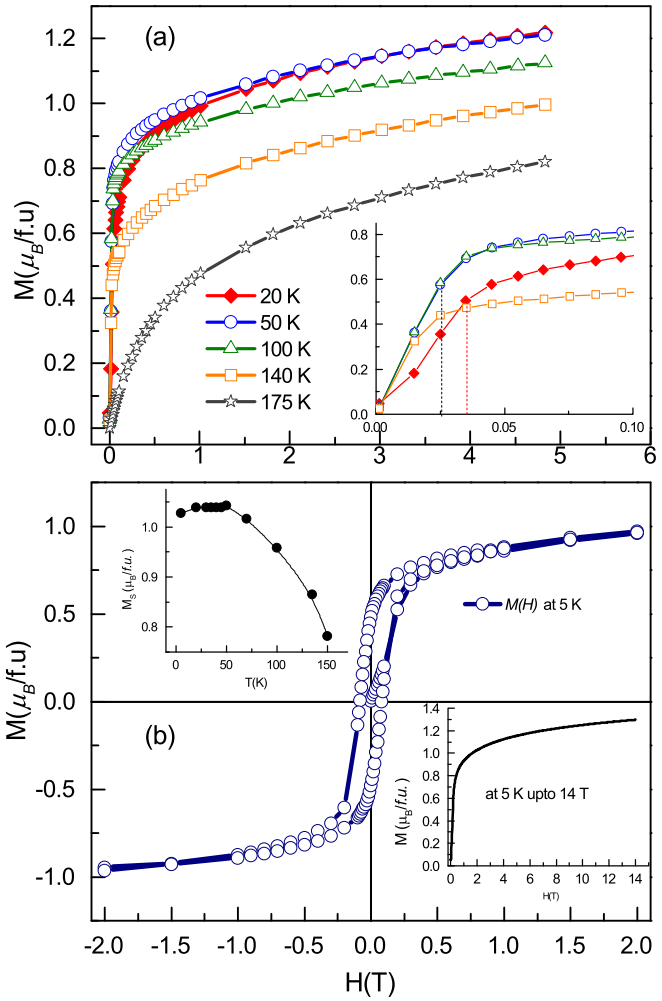

FIG. 2. Isothermal magnetization for Ga_2MnCo recorded at different temperatures. (a) $M(H)$ curves up to a field of 5 T at 20–175 K. Inset: magnified view of the $M(H)$ curves (up to 0.1 T). (b) Magnetic hysteresis loop of Ga_2MnCo at 5 K, and $H = 2$ T. Left inset: variation of the magnetic saturation moment recorded at different temperatures. Right inset: $M(H)$ curve for Ga_2MnCo at 5 K and H up to 14 T.

5.828 Å. To circumvent the problem of low intensity of the superlattice reflections in the XRD pattern, we undertake a thorough structural investigation using neutron diffraction, as discussed later in the text.

Next, we study the magnetic properties of Ga_2MnCo through dc magnetization measurement carried out as a function of temperature and applied magnetic field. Magnetization as a function of temperature [$M(T)$] recorded in an applied field of 100 Oe, following the zero-field-cooled-warming (ZFCW), field-cooled-cooling (FCC), and field-cooled-warming (FCW) protocols, is shown in Fig. 1(b). A signature of ferromagnetic ordering is seen at $T_C = 154$ K, followed by an abrupt downturn in $M(T)$ below 50 K, hinting a crossover to an antiferromagnetic order. We label this second transition as T_s. A clear bifurcation in the ZFCW-FC curve occurs in this low-temperature region, indicating nonergodicity in the $M(T)$ behavior of Ga_2MnCo below T_s. Figure 2(a) shows the dc magnetization measurement with the field variation, $M(H)$, recorded at different temperatures spanning T_C and T_s. All the $M(H)$ plots recorded at temperatures below T_C are quick to attain near-saturation values at a relatively smaller applied field of ∼0.1 T. Comparatively, curves recorded at temperatures below T_s show a sluggish buildup toward saturation [see the inset of Fig. 2(a)]. Overall, the saturation values, M_s, estimated by extrapolating $M(H)$ to $H = 0$, seem to increase systematically below T_C and attain a stable value below T_s. This observation is represented in the left inset of Fig. 2(b).

Importantly, as can be seen in Fig. 2(b), the $M(H)$ at 5 K shows considerable hysteresis, like a ferromagnet, but it does not saturate even under an applied field of 14 T, shown in the right inset of 2(b). Due to the presence of AFM interactions, a portion of the atomic moments is aligned antiparallel to the direction of spontaneous magnetization. Rotation of these moments in large magnetic fields determines the linear dependence of magnetization above saturation. The total saturation moment at 5 K, estimated by extrapolating this $M(H)$ to $H = 0$, is $1.12\mu_B$/f.u. and matches with the reported value of $1.34\mu_B$ recorded by Refs. [7,8]. However, this observed value differs considerably from the value calculated using the Slater-Pauling rule [15]. Here, the saturation magnetization is estimated using a simple relation, $M_S = (N - 24)$, where N represents the total number of valence electrons present in the system. Following this expression, the saturation magnetic moments obtained for stoichiometric Co-Mn-Ga alloys, viz. Co_2MnGa and Mn_2CoGa, turn out to be $4\mu_B$ and $2\mu_B$, and they agree with the experimentally reported [8] values of $4.14\mu_B$ and $2.1\mu_B$, respectively, while the experimental value for Ga_2MnCo seems to deviate from its estimate of $2\mu_B$, suggesting that a relook at the magnetic interactions in Ga_2MnCo is warranted.

Complex magnetic interactions below T_s, different from the one in the region $T_s \leqslant T \leqslant T_C$, might exist in Ga_2MnCo, which requires further explorations. With this aim, we undertook a powder neutron diffraction study of Ga_2MnCo at various temperatures ($6 \leqslant T \leqslant 300$ K) spanning all its magnetic transitions. The raw diffraction patterns are presented in Fig. 3. First, no extra peaks are observed in the diffraction patterns recorded below T_s, ruling out any long-range AFM order. Also, no signature of any structural distortions is evident from any of the patterns. The quantitative analysis carried out using the Rietveld refinement method and implemented through the FULLPROF suite [16] reaffirms the $Fm\bar{3}m$ symmetry in the crystal structure. Representative fits for diffraction patterns at 6 and 300 K are shown in Fig. 4. The unit-cell parameter at room temperature is found to be 5.829 Å, in agreement with the XRD data.

Unlike x rays, scattering with neutrons allows much better differentiation of site occupancy of the constituent atoms since the nuclear coherent scattering amplitudes of Co and Mn are widely different. We observe that a good match between the recorded data and the calculated profile is obtained, albeit after inclusion of ∼10% of site swapping between Mn and Co Wyckoff positions. Refinement of the data using site disorder of Ga atoms with Mn/Co was also explored, but it yields a poor fit to the experimental data. As the diffraction patterns are analyzed with respect to changing temperature, the intensity of low-angle reflections shows an appreciable increase below $T_C = 154$ K due to the FM long-range order. Below T_C, the

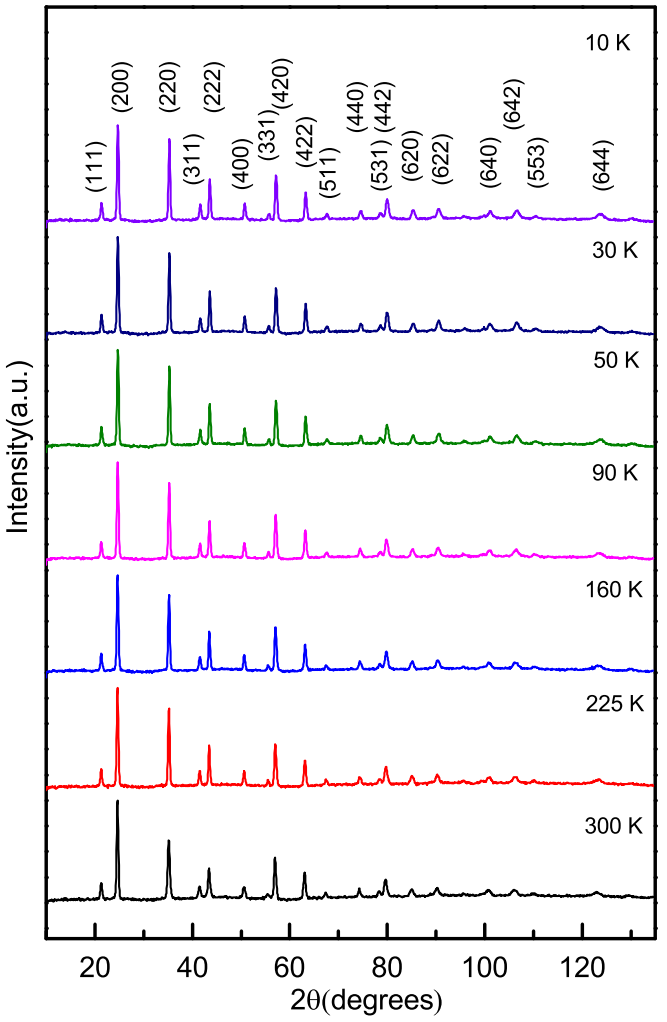

FIG. 3. ND pattern of Ga_2MnCo at various temperatures.

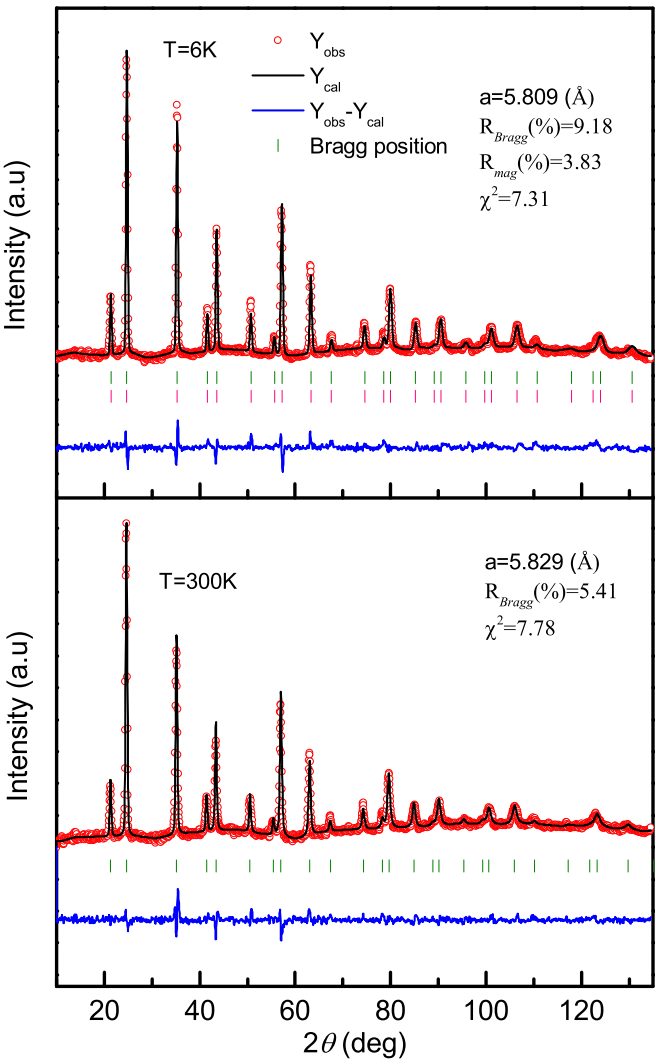

FIG. 4. The Rietveld refinement of the ND pattern of Ga_2MnCo at 6 and 300 K. Experimental data are represented by open circles, the calculated profile by a continuous line, and the allowed structural and magnetic Bragg reflections by vertical marks. The difference between the experimental and calculated profiles is displayed at the bottom of the graph.

refinement of the powder diffraction data has been carried out taking into account both the nuclear and magnetic phases. The parameters varied are scale, cell, background, moments on Co and Mn, and overall thermal parameters. The magnetic structure is found to be FM below T_C with a magnetic moment of $0.8(0.1)\mu_B$ and $0.6(0.1)\mu_B$ on Mn and Co, respectively, at 6 K. However, the temperature variation of the moment obtained from ND does not show the drop in magnetization below 50 K in $M(T)$. Also, no superlattice reflection corresponding to long-range AFM order appears below 50 K. Therefore, combining magnetization and neutron diffraction studies, we conclude that the long-range FM order that develops below T_C is hampered due to the development of some short-ranged AFM correlations below 50 K, giving rise to a situation like that of a cluster glass phase.

To obtain a rough estimate of the size of such FM clusters, we carried out a neutron depolarization experiment on the same powdered sample. Polarization is simply related to the Larmor precision of the neutron spin around the magnetic induction B in the sample. In the paramagnetic state, the spin fluctuates over a very short time scale compared to the typical Larmor time for the precession, and the neutron spins do not follow the $B(t)$ variation. Therefore, no depolarization is observed. Similarly, a spin-glass state with an atomic level of magnetic inhomogeneity also does not depolarize the neutron beam as $B(t)$ averages out to zero on a spatial scale, whereas the incident neutron gets depolarized by traversing through randomly oriented domains as in a typical ferromagnet. This technique for studying FM domains was initiated by Halperin and Holstein [17], and it has been able to provide useful information on the magnetic inhomogeneity with mesoscopic length-scale, like, spin clusters that carry a net moment.

The temperature dependence of neutron beam polarization in Ga_2MnCo was recorded across its paramagnetic, FM, and low-temperature phase. The measurement was performed in a FCW scan where the sample was cooled under an external field of 33 Oe and the data were recorded while warming. As can be seen from Fig. 5, with the decrease in temperature the polarization starts decreasing sharply below 160 K, signifying the onset of long-range FM order. Thereafter, a plateaulike

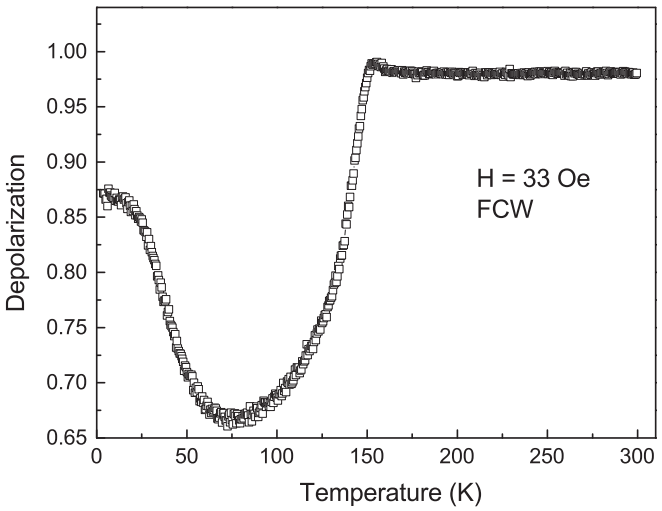

FIG. 5. Temperature dependence of the transmitted neutron polarization in $H = 33$ Oe.

region appears in the region between ∼128 and ∼50 K. This entire trend in polarization resembles a mirror image of the $M(T)$ measurement recorded in FC mode. Below 50 K, the polarization again increases, denoting either a weakening of domain size or domain magnetization. It should be noted that the polarization does not recover to its paramagnetic value, hence long-range ferromagnetic order is not lost. As seen from the inset to Fig. 2(b), the spontaneous magnetization does not decrease below ∼50 K. Therefore, the increase in polarization below 50 K could be due to weakening of the domain size.

An estimate of the domain size in the ferromagnetically ordered region of temperature can be obtained from the expression

$$P_f = P_i \exp\left[-\alpha\left(\frac{d}{\Delta}\right)\langle\Phi_\delta\rangle^2\right],$$

where P_i and P_f are initial and final beam polarization, α is a dimensionless parameter set to $1/3$, d is the sample thickness, Δ is the typical domain size, $\Phi_\delta = (4.63 \times 10^{-10}\ \mathrm{G^{-1}\,\AA^{-2}})\lambda B\Delta$ is the precession angle, and λ is the neutron wavelength. The bulk magnetization values presented in Fig. 2 are used here to obtain the domain magnetization B. Using the above expression, we obtain an average domain size of ∼2 μm at 75 K. However, it should be noted that the value quoted here is a fairly close estimate, and evaluation of a more accurate value would require a precise determination of B and three-dimensional polarization analysis [18]. Nevertheless, it is seen that large FM domains exist in Ga_2MnCo, indicative of long-range magnetic order, and a transition below 50 K shortens the domain size. To sum up, the neutron diffraction and magnetization measurement indicate that the long-range FM interactions that develop below 154 K are interrupted and their spatial extent shortened by some AFM interactions that develop below 50 K. Thus large FM clusters are connected via short-range oppositely aligned magnetic linkages.

To gain better insight into the origin of the second magnetic transition seen at T_s, low-field ac susceptibility was measured. The temperature dependence of χ_{ac} was recorded at different

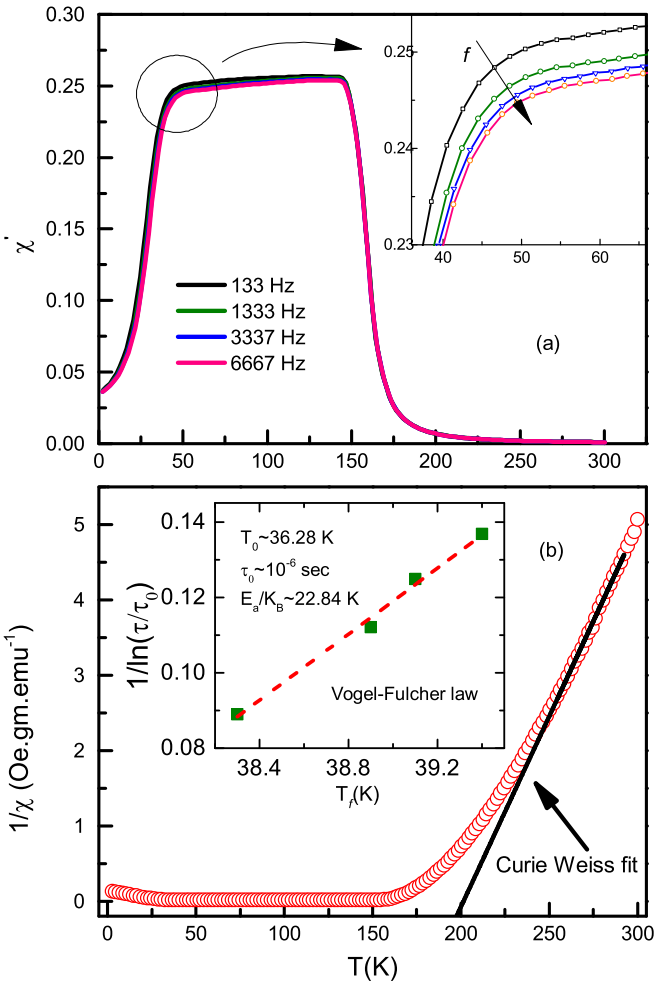

FIG. 6. Upper panel shows the temperature dependence of the real part of the ac susceptibility measured for Ga_2MnCo between 2 and 300 K, at different frequencies. The inset shows the magnified view of the χ at T_f. The lower panel shows a Curie-Weiss fit to the susceptibility of Ga_2MnCo. Inset: the variation of the freezing temperature T_f with the frequency of the ac field in a Vogel-Fulcher plot with $\tau = 10^{-6}$. The dashed line is the fit to the Vogel-Fulcher equation.

frequencies (f) ranging from 133 to 6667 Hz. Figure 6(a) shows the real component of the ac susceptibility (χ'_{ac}), where the overall trends and transition temperatures match with the previously stated dc $M(T)$ measurement. What is important to note is that the feature associated with T_s shifts toward higher temperature as the frequency changes from 133 to 6667 Hz. We observe a change in temperature values from 38.3 K at 133 Hz to 39.5 K at 6667 Hz. The frequency dependence of T_s, though weaker, is similar to that of a Ruderman-Kittel-Kasuya-Yosida (RKKY) spin system [19]. In the lower panel of Fig. 6, a linear fit to the inverse susceptibility curves yields $\theta_{CW} = 198$ K, a value much greater than T_C (=154 K), which suggests that the spins begin to align locally well before a long-range FM order is realized. This observation also clarifies the curvature in the $M(H)$ recorded at 175 K [see Fig. 2(a)] in contrast to a typical paramagnetic state.

The frequency-dependent shift in T_s gives a clear indication of a glassy magnetic phase being present at low temperature in Ga_2MnCo. Rather, to be more apt, T_s signifies the onset of a reentrant spin glass (RSG) in Ga_2MnCo as the glassy state emerges after the system has ordered in a stable FM state [14,20]. The flat topped humplike feature at T_s, seen in the χ'_{ac} versus T curve, is suggestive of the critical concentration of magnetic entities for percolation of ferromagnetism [21]. A frequency-dependent shift in the temperature associated with this feature is indicative of the formation of clusterlike entities of varying sizes, and the temperature itself can be associated with the spin freezing temperature, T_f. The spin freezing/blocking process is defined by $\phi = \Delta T_f/[T_f \Delta \log_{10}(f)]$, and ϕ varies from approximately 0.005 to 0.05 depending on the systems [12]. For a well-known canonical spin glass such as CuMn, ϕ is estimated to be 0.005. For Ga_2MnCo, ϕ works out to be 0.017, indicating a much larger sensitivity to the frequency and qualifying it to be classified in the cluster glass regime [22].

To further verify the cluster glass state in Ga_2MnCo, a logarithmic frequency dependence of the freezing temperature that follows Vogel-Fulcher empirical law is proposed. As per this law, $\tau = \tau_0 \exp[\frac{E_a}{k_B(T_f - T_0)}]$, where τ_0 is the characteristic time, and E_a and T_0 are the activation energy and the Vogel-Fulcher temperature, respectively, which give the intercluster interaction strength. The inset to Fig. 6(b) shows the Vogel-Fulcher plot for Ga_2MnCo along with the extracted values for E_a/K_B, T_0, and the characteristic time τ_0. The data for Ga_2MnCo give a τ_0 value of 10^{-6} s, which is much higher than that obtained for conventional spin glasses ($\sim 10^{-12}$–10^{-10} s) [12]. Such a value of the characteristic time, which is also found in RSG systems such as $Ni_2Mn_{1.36}Sn_{0.64}$ [23], suggests a slow spin dynamics in Ga_2MnCo due to the cluster formation. The values of E_a/K_B and T_0 are found to be 22.84 and 36.28 K, respectively. T_0 is very close to the value of the spin freezing temperature obtained from linear ac susceptibility measurements, indicating that the RKKY interaction is relatively strong in this compound. The Tholence criterion [19] $t^* = \frac{(T_f - T_0)}{T_f}$ for Ga_2MnCo works out to be 0.052. Altogether these observations clearly suggest that the spin-glass state in Ga_2MnCo is related to the FM cluster formation and falls in a category of a RKKY spin-glass system.

IV. DISCUSSIONS

Neutron diffraction revealed that the Ga_2MnCo lattice maintains a cubic structure over the entire temperature range, and the variation of the lattice parameter with temperature is plotted in the lower panel of Fig. 7. These values are found to vary from 5.8095(3) Å at 6 K to 5.8294(4) Å at 300 K. Surprisingly, an abrupt change of about 0.1% is found in the lattice parameter around the cluster glass phase transition, 50 K. Beyond 50 K, the lattice undergoes normal thermal expansion with increasing temperature.

Although the degree of lattice expansion at T_s is small, we tried to find evidence of it, if any, in the transport properties of Ga_2MnCo. Toward that end, the electrical resistance was measured by varying the temperature of the sample, as depicted in Fig. 7. Conventional metallic conduction behavior, i.e., $\frac{dR}{dt} > 0$, is observed throughout the measured temperature

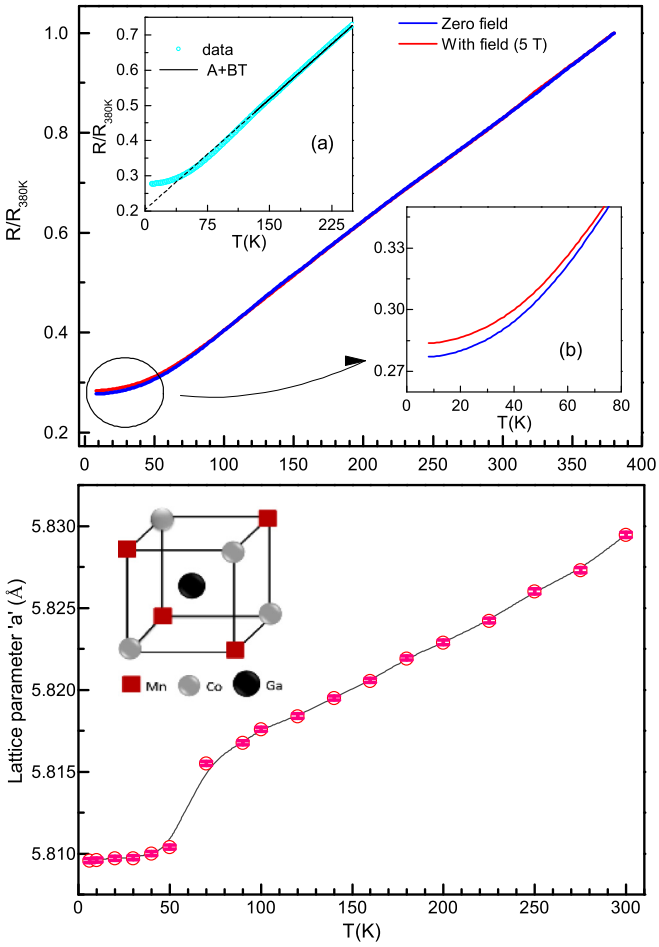

FIG. 7. Upper panel: Dependence of normalized resistance as a function of temperature, with and without the presence of a magnetic field. The left inset (a) shows the phonon contribution. The right inset (b) shows the magnified view of the resistance plot at low temperatures. Lower panel: The lattice parameter variation with temperature as obtained from refining the ND data. The inset shows the $L1_0$ configuration containing the magnetic ions.

range. The data seem to follow a typical phonon dependence ($\propto T$) for most of the temperature range: 380–130 K. Below 130 K ($< T_C$), the slope of the curve starts to change slightly as the electron-electron interaction and magnetic correlation effects become significant. No sign of any anomaly related to the lattice distortion at T_s is observed. Application of a sufficiently high magnetic field of 5 T leads to about a 2.5% increase in the resistance below T_s (see the inset to Fig. 7).

Although there is no symmetry breaking transition witnessed from neutron diffraction measurement, the cell volume expansion at the cluster glass-transition temperature indicates a correlation of magnetic and crystal structural degrees of freedom. The origin of such an anomaly should lie in the $\sim$10% disorder in the site occupancy of Co and Mn crystallographic positions, encountered during refinement of neutron diffraction profiles. We believe the presence of this site disorder decides the extremity of the magnetic interactions, which leads to the associated cluster glass state. The inset of Fig. 7 (lower panel) presents a schematic of the $L1_0$

subcell of magnetic atoms in Ga_2MnCo that forms part of the larger $L2_1$ unit cell. In the ideal lattice scenario, Mn atoms have Co as their nearest-neighbor (NN) magnetic atoms and other Mn atoms present along the face diagonal as their next nearest neighbors (NNN). This NNN Mn-Mn interaction is FM in nature and orders below 154 K, as witnessed from the magnetization and neutron diffraction measurement. The nonmagnetic Ga atom sits at the body-centered position in the subcell.

Our results suggest that when one of these NN Co atoms swaps positions with Mn, we have a situation with a new NN correlation identified as Mn-Mn′. The swapped Mn′ atom finds itself in an already existing FM order between the NNN Mn-Mn. As the magnetic interactions in Heusler alloys are mediated via RKKY-type exchange interactions, the Mn-Mn interactions are predominantly influenced by the distance between them. This fact has been demonstrated using first-principles calculations [1], as well as by using Monte Carlo simulations [24], in $Ni_2Mn_{1+x}Z_{1-x}$. Moreover, EXAFS and XMCD studies [25,26] on $Ni_2Mn_{1.4}In_{0.6}$ also demonstrate the significance of bond distance in dictating its magnetic interactions. Hence the new NN Mn-Mn′ interactions in Ga_2MnCo are AFM in nature. As the temperature is lowered, the lattice begins to contract and the as of yet neglected NN interactions begin to gain relevance, setting the stage for a competition between magnetic interactions. However, the number of new NN AFM pairs is much lower (in the present case, ∼10% site disorder) compared to the FM pairs. Overall, a ferromagnetic order gets established in large spatial regions of the sample, with disorder-induced AFM linkages between these spatial regions. The long-range FM spin symmetry throughout the bulk sample is thus disturbed, giving rise to a cluster glass situation at low temperature.

V. CONCLUSIONS

We studied the structural, magnetic, and electrical transport properties of the Ga_2MnCo Heusler alloy. Insights gained from neutron diffraction and ac susceptibility measurements help us to determine the magnetic ground state of this system. All the evidence suggests a cluster glass phase at low temperature and a ferromagnetic state at high temperature. The competing interactions between Mn atoms that administer a ferromagnetic-type ordering at higher temperature form large clusters of FM interjected by tiny AFM interactions at low temperatures. The corresponding unusual distortion in the lattice, without a change in symmetry, is seen at the cluster-glass transition. The site occupancies of magnetic atoms in the crystal structure play the critical role in controlling its low-temperature magnetic ground state.

ACKNOWLEDGMENTS

T.S. and P.A.B. gratefully acknowledge support from the Department of Science and Technology (DST), New Delhi under Project No. SR/S2/CMP-0109/2012. We thank Devendra Buddhikot (TIFR) for help in the measurement of transport and magnetic properties, and Ripandeep Singh (BARC) for help with neutron measurement. P.A.B. also thanks the DST, India for the financial support and Saha Institute of Nuclear Physics, India for facilitating the experiments at the Indian Beamline, Photon Factory, KEK, Japan.

[1] J. Kübler, A. R. Williams, and C. B. Sommers, Phys. Rev. B **28**, 1745 (1983).
[2] M. Meinert, J.-M. Schmalhorst, C. Klewe, G. Reiss, E. Arenholz, T. Böhnert, and K. Nielsch, Phys. Rev. B **84**, 132405 (2011).
[3] R. Stinshoff, A. K. Nayak, G. H. Fecher, B. Balke, S. Ouardi, Y. Skourski, T. Nakamura, and C. Felser, Phys. Rev. B **95**, 060410 (2017).
[4] W. Zhang, Y. Sun, H. Wang, Y. Li, X. Zhang, Y. Sui, H. Luo, F. Meng, Z. Qian, and G. Wu, J. Alloys Compd. **589**, 230 (2014).
[5] S. R. Barman, A. Chakrabarti, S. Singh, S. Banik, S. Bhardwaj, P. L. Paulose, B. A. Chalke, A. K. Panda, A. Mitra, and A. M. Awasthi, Phys. Rev. B **78**, 134406 (2008).
[6] H. Shiraishi, T. Hori, and Y. Yamaguchi, J. Magn. Magn. Mater. **104-107**, 2040 (1992).
[7] J. Chen, E. Liu, X. Qi, H. Luo, W. Wang, H. Zhang, S. Wang, J. Cai, and G. Wu, Comput. Mater. Sci. **89**, 130 (2014).
[8] G. J. Li, E. K. Liu, Y. J. Zhang, Y. Du, H. W. Zhang, W. H. Wanga, and G. H. Wu, J. Appl. Phys. **113**, 103903 (2013).
[9] F. A. Hames, J. Appl. Phys. **31**, S370 (1960).
[10] V. Alijani, J. Winterlik, G. H. Fecher, and C. Felser, Appl. Phys. Lett. **99**, 222510 (2011).
[11] H. Shiraishi, M. Sugamura, and T. Hori, J. Magn. Magn. Mater. **70**, 230 (1987).
[12] J. A. Mydosh, Rep. Prog. Phys. **78**, 052501 (2015).
[13] D. Hüser, M. J. F. M. Rewiersma, J. A. Mydosh, and G. J. Nieuwenhuys, Phys. Rev. Lett. **51**, 1290 (1983).
[14] L. Ma, W. H. Wang, J. B. Lu, J. Q. Li, C. M. Zhen, D. L. Hou, and G. H. Wu, Appl. Phys. Lett. **99**, 182507 (2011).
[15] I. Galanakis, P. H. Dederichs, and N. Papanikolaou, Phys. Rev. B **66**, 174429 (2002).
[16] J. Rodriguez-Carvajal, Physica B: Condens. Matter **192**, 55 (1993).
[17] O. Halpern and T. Holstein, Phys. Rev. **59**, 960 (1941).
[18] A. Das, S. K. Paranjpe, S. Honda, S. Murayama, and Y. Tsuchiya, J. Phys.: Condens. Matter **11**, 5209 (1999).
[19] J.-L. Tholence, Physica B+C **126**, 157 (1984).
[20] K. Motoya, S. Kubota, and K. Nakaguchi, J. Phys. Soc. Jpn. **68**, 2351 (1999).
[21] B. Coles, B. Sarkissian, and R. Taylor, Philos. Mag. B **37**, 489 (1978).
[22] J. A. Mydosh, *Spin Glasses: An Experimental Introduction* (Taylor and Francis, London, 1993).
[23] S. Chatterjee, S. Giri, S. K. De, and S. Majumdar, Phys. Rev. B **79**, 092410 (2009).
[24] V. D. Buchelnikov, P. Entel, S. V. Taskaev, V. V. Sokolovsky, A. Hucht, M. Ogura, H. Akai, M. E. Gruner, and S. K. Nayak, Phys. Rev. B **78**, 184427 (2008).
[25] K. R. Priolkar, D. N. Lobo, P. A. Bhobe, S. Emura, and A. K. Nigam, Europhys. Lett. **94**, 38006 (2011).
[26] K. R. Priolkar, P. A. Bhobe, D. N. Lobo, S. W. D'Souza, S. R. Barman, A. Chakrabarti, and S. Emura, Phys. Rev. B **87**, 144412 (2013).